Available online at www.sciencedirect.com
ScienceDirect
Polymer 48 (2007) 7113–7120
polymer
www.elsevier.com/locate/polymer

Gelation and degradation characteristics of *in situ* photo-crosslinked poly(L-lactide-*co*-ethylene oxide-*co*-fumarate) hydrogels

Alireza S. Sarvestani, Weijie Xu, Xuezhong He, Esmaiel Jabbari*

Biomimetic Materials and Tissue Engineering Laboratories, Department of Chemical Engineering, University of South Carolina, Columbia, SC 29208, United States

Received 21 August 2007; received in revised form 4 October 2007; accepted 5 October 2007
Available online 11 October 2007

Abstract

The objective of this work was to determine the gelation kinetics, extent of swelling, sol fraction, and degradation kinetics of photo-crosslinked poly(L-lactide-*co*-ethylene oxide-*co*-fumarate) (PLEOF) hydrogels, with *N*-vinyl-2-pyrrolidone (NVP) crosslinker, as a function of composition as well as the time and intensity of UV radiation. The gelation process was monitored by *in situ* rheometry. The crosslinking was shown to be facilitated by increasing NVP concentration up to a certain value above which the hydrogel shear modulus did not increase with additional amount of NVP. Increasing the hydrophobicity of PLEOF macromer resulted in a decrease in the hydrogel swelling ratio and increase in sol fraction which was due to a reduction in the apparent reactivity of the PLEOF fumarate units. The degradation characteristics of PLEOF hydrogels depended on the ratio of PLA to PEG with PLEOF 30/70 (30% lactide) having the highest degradation rate.

Keywords: Hydrogel; Biodegradable; *In situ* gelation kinetics

1. Introduction

Hydrogels are three-dimensional crosslinked polymeric structures which are able to swell in physiological solution and retain a significant fraction of water in their structure without dissolving [1–4]. Small hydrophilic nutrient molecules can readily diffuse through hydrogels [5,6]. In addition, diffusivity of macromolecules and proteins in hydrogels is 4–5 orders of magnitude higher compared to glassy polymers [7,8] and cells immobilized in hydrogels are more likely to retain their biological activity than hydrophobic polymers [9–12]. Hydrogels, due to their hydrophilicity and high permeability to oxygen and nutrients, are very attractive for cell encapsulation and soft tissue replacement [11,12], while those reinforced with calcium phosphate nanoparticles are useful for hard tissue regeneration [13–15]. Hydrogel precursor solutions can be crosslinked with bioactive peptides to produce smart cell-responsive hydrogels [16–18]. Hydrogels are also used for fabrication of non-biofouling micro and nanochannels in two-dimensional surface patterning and three-dimensional device fabrication [19].

Temperature, pH, photo-sensitive compounds, and reducing agents are used to initiate the crosslinking reaction [20]. Since biological systems have a narrow range of acceptable temperature and pH and low tolerance for toxic compounds, photo-initiation is the most feasible method of hydrogel preparation for treating irregularly shaped defects [21–24]. Other advantages of photo-initiation include spatial and temporal control over the crosslinking reaction and fast polymerization rates at physiological temperature [25,26].

A number of *in situ* crosslinkable synthetic macromers have been developed for preparation of degradable hydrogels [27–30]. Promising results have been obtained with poly(ethylene) glycol (PEG) based macromers modified with reactive

* Corresponding author. Department of Chemical Engineering, Swearingen Engineering Center, Rm 2C11, University of South Carolina, Columbia, SC 29208, United States. Tel.: +1 803 777 8022; fax: +1 803 777 0973.
E-mail address: jabbari@engr.sc.edu (E. Jabbari).

0032-3861/$ - see front matter © 2007 Elsevier Ltd. All rights reserved.
doi:10.1016/j.polymer.2007.10.007

functional groups like methacrylate, acrylate, fumarate, and sulfide groups that can be injected and crosslinked *in situ* using redox initiators or ultraviolet (UV) light [31–36]. The results demonstrate that the hydrogel network structure, biocompatibility, degradation, and viscoelastic properties are affected by reaction conditions like component concentrations in the polymerizing mixture and chemical composition of the macromers [37–39]. For example, hydrogel crosslink density, which is directly related to the ultimate gel modulus and inversely related to water content, can be adjusted by the concentration of components in the polymerizing mixture. The extent of swelling, in turn, impacts permeability, degradation, cell viability, and viscoelastic properties [40].

In an attempt to control water content (hence mechanical strength), degradation rate, and the rate of crosslinking, our laboratory has developed a multi-functional poly(L-lactide-*co*-ethylene oxide-*co*-fumarate) (PLEOF) macromer consisting of ultra-low molecular weight poly(L-lactide) (ULMW PLA) and PEG blocks linked by unsaturated fumarate units [11]. The PLA and PEG are FDA approved and fumaric acid occurs naturally in the Krebs cycle [41]. The water content can be adjusted by the ratio of the hydrophilic PEG to hydrophobic PLA blocks and by the molecular weight of PEG. The degradation rate of the network can be tailored to a particular application by the ratio of PLA to PEG blocks or by using ULMW poly(lactide-*co*-glycolide) (PLGA) in place of ULMW PLA [42,43].

The gelation kinetics of the PLEOF hydrogel precursor solutions crosslinked with a neutral redox initiation system was investigated by us previously [44]. We proposed a kinetic model for radical polymerization of PLEOF and investigated the effect of each component of the precursor solution on the network structure, gelation kinetics, and ultimate shear modulus. The objective of this work was to investigate the effect of hydrogel composition on gelation kinetics, the extent of swelling, and degradation of PLEOF hydrogels crosslinked by ultraviolet (UV) radiation. The hydrogel precursor solution consisted of PLEOF macromer, *N*-vinyl-2-pyrrolidone (NVP) crosslinker, and 4-(2-hydroxyethoxy)phenyl-(2-hydroxy-2-propyl)ketone photo-initiator. The gelation kinetics was measured *in situ* by rheometry.

2. Experimental part

2.1. Macromer synthesis

PLEOF was synthesized by condensation polymerization of ULMW PLA and PEG with fumaryl chloride (FuCl) as described in detail in a previous publication [44]. The weight ratio of PLA to PEG was changed from 20/80 to 40/60 to produce PLEOF terpolymers with varying extent of swelling and hydrophilicity. The structure of the PLEOF macromer was characterized by ^{1}H NMR and GPC. The M_n and PI of 20/80 PLEOF were 8910 ± 150 Da and 1.7 ± 0.1, respectively, those of 30/70 PLEOF were 8010 ± 150 Da and 1.6 ± 0.1, and those of 40/60 PLEOF were 8060 ± 150 Da and 1.6 ± 0.1.

2.2. Hydrogel synthesis

Hydrogels were prepared by free-radical polymerization of the PLEOF macromer and NVP (Aldrich, Milwaukee, WI) crosslinker, with 4-(2-hydroxyethoxy)phenyl-(2-hydroxy-2-propyl)ketone (Irgacure 2959; Ciba, Tarrytown, NY) photo-initiator, in distilled deionized (DDI) water. The reaction scheme for photo-crosslinking is shown in Fig. 1. The photo-initiator was dissolved in NVP by heating the mixture to 50 °C. Next, PLEOF was dissolved in DDI water and the mixture was vortexed periodically and heated to aid dissolution. Then, NVP/initiator mixture was added to the aqueous PLEOF solution, the mixture was vortexed, and loaded on the Peltier plate of the rheometer. The hydrogel precursor solution was exposed to UV light, as described below, for time period $t_{UV} \leq 30$ min. The initiator was dissolved in *N*-methyl-2-pyrrolidone (NMP; Aldrich) for the formulations without NVP. The notation "*a*P–*b*N–*c*I" is used to identify the concentration of components in various hydrogel samples, where *a*, *b*, and *c* represent the mole percent of PLEOF, NVP, and photo-initiator in the hydrogel precursor solution, respectively. The results are for PLA:PEG ratio of 20/80, unless otherwise specified.

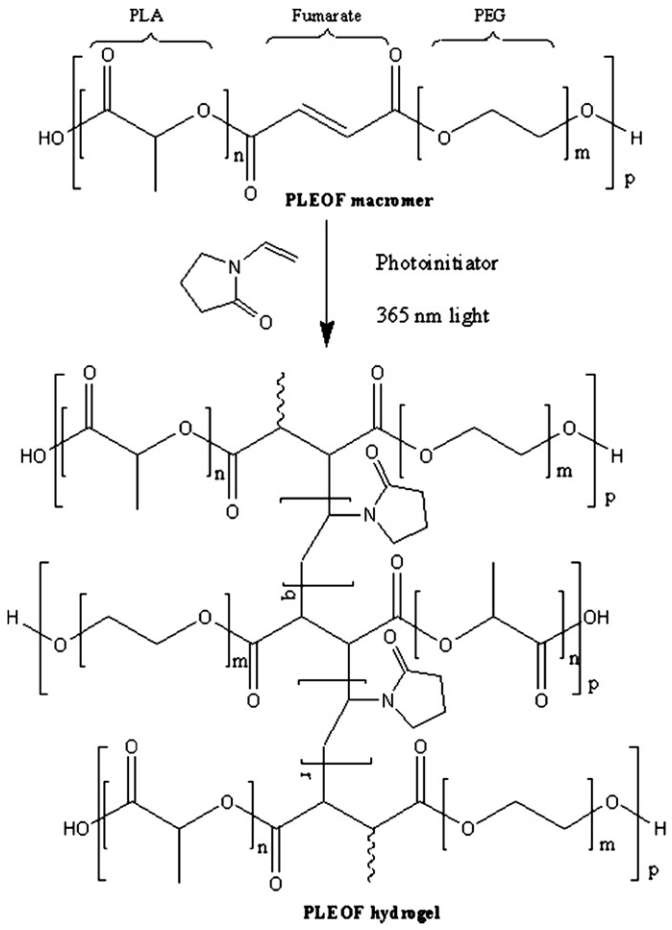

Fig. 1. The reaction scheme for photo-crosslinking of the PLEOF precursor solution.

2.3. Rheological measurements

Rheological measurements were performed at 37 °C on an AR-2000 rheometer (TA Instruments, New Castle, DE) equipped with a parallel plate geometry (acrylic plate transparent to UV light; 20 mm diameter; TA Instruments). A sinusoidal shear strain profile was exerted on the sample via the upper geometry at a constant frequency of 1 Hz. The deformation amplitude was 1% to remain within the linear region of viscoelasticity. The polymerizing mixture was injected on the Peltier plate and the upper geometry was lowered to a gap of 300 μm. The sample was irradiated with a BLAK-RAY 100-W mercury long wavelength (365 nm) UV lamp (Model B100-AP; UVP, Upland, CA) located at distance d from the center of the Peltier plate (Fig. 2). The elapsed time between mixing/injection and the start of data collection was 30 s for all experiments. The storage modulus (G') during the gelation process was monitored by the rheometer. The intensity of the transmitted UV light was measured by a BLAK-RAY long-wave ultraviolet radiation meter (Model J-221; UVP). The transparency of the acrylic geometry to long-wave (365) UV light was confirmed by comparing the intensity of the transmitted light through the geometry to that of the incident light (transmitted intensity was >95%). The measured UV intensity at a distance of 10, 30, 35, and 40 cm from the lamp was 46,000, 5300, 4000, and 3000 μW/cm^2, respectively. In the text, ''shear modulus'' is defined as the storage shear modulus of the hydrogel sample after 1800 s of UV radiation. All hydrogel samples reached a plateau shear modulus after 1800 s of irradiation.

2.4. Measurement of swelling ratio and sol fraction

After completion of the gelation experiments, crosslinked samples (20 mm diameter × 300 μm thickness) were removed from the Peltier plate to measure the swelling ratio and sol fraction. Samples were dried at ambient conditions for 12 h followed by drying in vacuum for 1 h at 40 °C and the total dry weight (W_i; sol plus gel) was recorded. Next, the dry samples were swollen in DDI water for 24 h at 37 °C with a change of swelling medium every 6 h. After swelling, sample was removed from the swelling medium, the surface water was removed, and the swollen weight, W_s, was recorded. Finally, the swollen sample was dried, as described above, and the dry gel weight, W_d, was recorded. The weight swelling ratio, Q, and the sol fraction, S, were calculated by the following equations:

$$Q = \frac{W_s - W_d}{W_d} \times 100, \quad (1)$$

$$S = \frac{W_i - W_d}{W_i} \times 100. \quad (2)$$

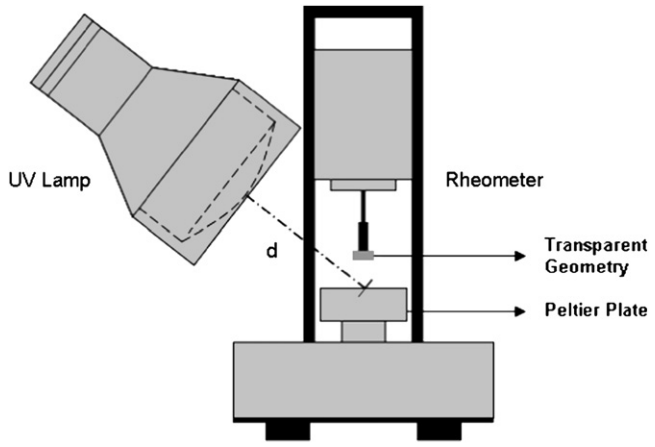

Fig. 2. Schematic diagram of the experimental set up for simultaneous *in situ* UV crosslinking and measurement of the shear modulus of PLEOF hydrogels with the rheometer.

2.5. Hydrogel degradation

The hydrogel precursor solution was prepared as described above, degassed, and transferred into a Teflon mold (3 cm × 5 cm × 750 μm), covered with a glass plate (the glass plate was transparent to UV), and fastened with clips, and irradiated with the UV lamp for 500 s. The distance between the radiation source and the sample was 10 cm. After crosslinking, the sample was removed from the mold and disks were cut from the gel using an 8 mm cork borer. Degradation was measured as a function of time in primary culture media (5 ml per sample) without fetal bovine serum (FBS) at 37 °C under mild agitation. To prepare the primary media without FBS, 13.4 g of Dulbecco's Modified Eagle Medium (DMEM; 4.5 g/l glucose with L-glutamine and without sodium pyruvate; Mediatech, Herndon, VA) was dissolved in 900 ml of DDI water containing 3.7 g sodium bicarbonate and 10 ml antibiotic and antimycotic agents (1% v/v). The antibiotic and antimycotic agents included 50 μg/ml gentamicin sulfate (GS; Sigma), 100 μg/ml streptomycin (Sigma), and 250 ng/ml fungizone. At each time point, samples were removed from the media, washed with DDI water to remove excess electrolytes, and dried in vacuum. The dry sample weight was recorded and compared with the initial dry weight to determine fractional mass remaining. The pH of the degradation media was measured with a Thermo Orion pH meter (Model 290; Orion Research, Boston, MA).

3. Results

The effect of initiator concentration on gelation kinetics of 18.0P–4.1N hydrogels is shown in Fig. 3. The rate of crosslinking was strongly dependant on the initiator concentration. The shear modulus also increased with the initiator concentration from 86 ± 21 kPa for 18.0P–4.1N–0.8I hydrogel to 181 ± 15 kPa for 18.0P–4.1N–1.6I. The effect of PLEOF concentration on the shear modulus of 4.1N–1.2I hydrogels is shown in Fig. 4(a). The modulus increased by approximately five folds as the PLEOF concentration increased from 14.4 to 21.6 mol%. The effect of NVP content on the

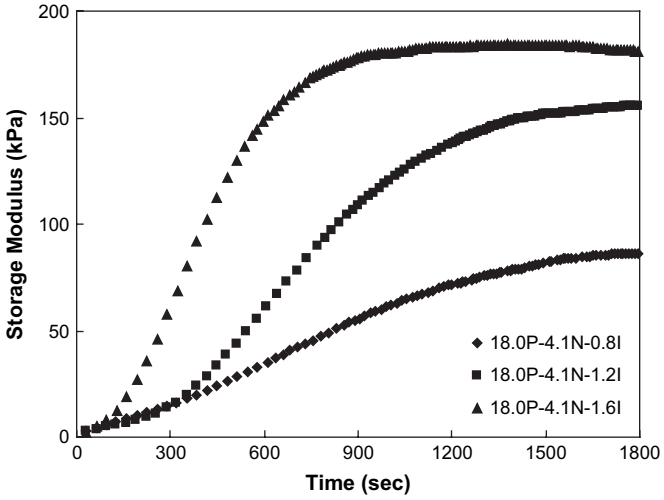

Fig. 3. Effect of UV initiator concentration on the time evolution of storage modulus of 18.0P–4.1N hydrogels ($d = 10$ cm and $t_{UV} = 30$ min).

shear modulus is shown in Fig. 4(b). The modulus initially increased with NVP concentration and then it decreased for the concentrations greater than 4.1 mol%. For similar initiator and PLEOF concentrations, hydrogels prepared without NVP had the lowest modulus. Fig. 4(c) shows the effect of PLA:PEG ratio on the shear modulus of 8.0P–4.1N–1.2I hydrogels. The shear modulus decreased sharply as the PLA fraction was increased. The final storage modulus for PLEOF with PLA:PEG = 20/80 was 155 ± 23 kPa, while that of PLA:PEG = 40/60 was lower by one order of magnitude (14 ± 5 kPa).

The effect of UV intensity and irradiation time on the shear modulus was investigated with 18.0P–4.1N–1.2I hydrogel. Table 1 shows the values of the shear modulus as a function of UV intensity after 30 min of irradiation. The intensity, which was proportional to d^{-2}, was varied by changing d, the distance between the UV lamp and the center of the Peltier plate. The shear modulus increased significantly as the intensity was increased from 3000 to 4000 μW/cm^2, but the increase was less dramatic when the intensity was changed from 5300 to 46000 μW/cm^2. Table 2 shows the values of the shear modulus of 18.0P–4.1N–1.2I hydrogel as a function of UV exposure time.

The effects of initiator and PLEOF concentrations on swelling and sol fraction of the hydrogels are shown in Fig. 5(a and b), respectively. These results show a decreasing trend in the values of sol fraction with increasing initiator concentration. This can be attributed to the enhancement in radical production with increasing initiator content [45,46]. The swelling ratio of the hydrogels initially decreased as the initiator concentration was raised from 14.4 to 18.0 mol%, but it remained unchanged in the range of 18.0–21.6 mol%. The swelling ratio and sol fraction did not change appreciably, within the range of experimental errors, with increasing PLEOF concentration from 14.4 to 21.6 mol% (Fig. 5(b)).

Fig. 5(c) shows the effect of NVP concentration on the sol fraction and swelling ratio. Hydrogels crosslinked without

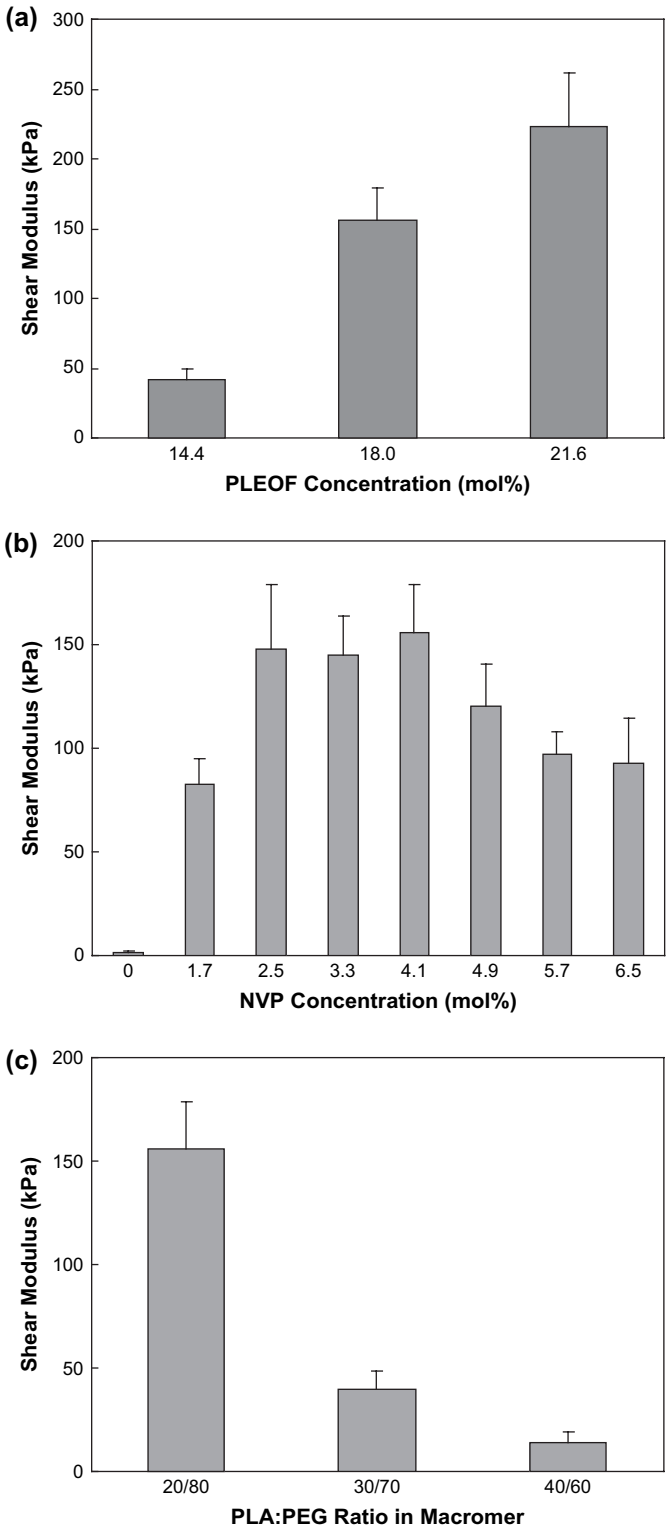

Fig. 4. Variation of the shear modulus with (a) PLEOF concentration in 4.1N–1.2I hydrogels, (b) NVP concentration in 18.0P–1.2I hydrogels, and (c) PLA:-PEG ratio in 18.0P–4.1N–1.2I hydrogels ($d = 10$ cm and $t_{UV} = 30$ min). The values reported are the mean of four samples with error bars representing one standard deviation from the mean.

Table 1
Effect of UV intensity on the shear modulus, swelling ratio, and sol fraction of 18.0P–4.1N–1.2I hydrogel ($t_{UV} = 30$ min)

	Intensity ($\mu W/cm^2$)			
	46,000	5300	4000	3000
Shear modulus (kPa)	155 ± 23	125 ± 20	119 ± 14	44 ± 8
Swelling ratio (%)	268 ± 23	297 ± 11	293 ± 7	361 ± 8
Sol fraction (%)	35 ± 3	42 ± 2	41 ± 1	49 ± 8

NVP crosslinker had the highest sol fraction and swelling ratio, demonstrating that PLEOF chains did not effectively participate in the crosslinking reaction in the absence of NVP. Swelling ratio decreased with increasing NVP concentration below 4.9 mol%. This trend was reversed for NVP concentrations above 5.7 mol%. Sol fraction decreased with increasing NVP concentration below 2.5 mol% and remained practically constant (within the range of error bars) for concentrations above 2.5 mol%. Increasing the hydrophobicity of PLEOF macromers (higher PLA fractions in the chains) decreased the swelling ratio and significantly enhanced sol fraction of the hydrogels, as shown in Fig. 5(d). Therefore, high PLA fractions in the macromer reduced the apparent reactivity of the PLEOF fumarate units with the growing NVP chains or other fumarate units.

The effect of UV intensity on the swelling ratio and sol fraction of 18.0P–4.1N–1.2I hydrogel is shown in Table 1. Swelling ratio and sol fraction were inversely proportional to UV intensity. UV exposure time had a similar effect on the swelling ratio and sol fraction of 18.0P–4.1N–1.2I hydrogel, as shown in Table 2. Samples which were exposed to UV for 3 min showed the lowest swelling ratio which was due to the low degree of crosslinking, resulting in a high sol fraction. The degradation characteristics of PLEOF hydrogels for different PLA:PEG ratios as a function of time are shown in Fig. 6. The results show that the degradation rate of PLEOF networks depends strongly on the PLA content and it can be controlled by varying the PLA:PEG ratio.

4. Discussion

The increase in shear modulus and decrease in swelling ratio at higher initiator concentrations implied that hydrogel crosslink density increased with initiator concentration. Assuming Gaussian distribution of chain lengths between crosslinks, average molecular weight between crosslinks, $\overline{M}_c$, can be obtained by [47]:

Table 2
Effect of UV irradiation time on the swelling ratio and sol fraction of 18P–4.1N–1.2I hydrogel ($d = 10$ cm)

	Exposure time (min)			
	30	10	7	3
Shear modulus (kPa)	155 ± 23	102 ± 12.8	44.9 ± 5.1	5.2 ± 1.7
Swelling ratio (%)	268 ± 23	297 ± 11	323 ± 15	243 ± 18
Sol fraction (%)	35 ± 3	40 ± 2	45 ± 8	65 ± 6

$$\overline{M}_c = RT\frac{\rho(1-S)}{G'}, \tag{3}$$

where ρ is the mass density of PLEOF macromers (900 kg/m^3), G' is the shear modulus (Pa), R is the gas constant (8.31 J/mol K), T is the absolute temperature (310 K), and S is the sol fraction. Using Eq. (3), $\overline{M}_c$ decreased from 17.3 ± 5.6 to 9.7 ± 1.7 and 8.9 ± 0.8 kDa as the initiator concentration was increased from 0.8 to 1.2 and 1.6 mol%, respectively. The $\overline{M}_c$ values are consistent with the swelling results, i.e., the swelling ratio did not change significantly for hydrogels with initiator concentrations in the range of 1.2–1.6 mol% (Fig. 5(a)).

Assuming steady-state assumption of the radicals, the radical concentration or the concentration of the growing chains, [R], is given by [48]:

$$[\mathrm{R}] = \left[\frac{2\phi I_0 \delta[\mathrm{I}]}{K_t}\right]^{1/2}, \tag{4}$$

where K_t and ϕ are the termination rate constant and photoinitiation efficiency, respectively, I_0 is the incident radiation intensity, δ is the sample thickness, and [I] is the initiator concentration. The kinetic chain length, which is the ratio of the propagation rate to the initiation rate, is given by:

$$L = \frac{K_p}{(2\phi I_0 \delta K_t)^{1/2}}\frac{[\mathrm{M}]}{[\mathrm{I}]^{1/2}}, \tag{5}$$

where K_p is the rate constant for propagation and [M] is the monomer concentration. These equations show that, at constant UV intensity, the number of growing radicals increases with square root of initiator concentration while the kinetic chain length (average length of the growing chains) is directly related to the monomer concentration, [M], and inversely related to the square root of initiator concentration, [I]. At constant PLEOF and NVP concentrations, as the initiator is increased, the kinetic chain length is decreased while the number of growing chains, [R], is increased. The radicals formed by the dissociation of the initiator react with a NVP monomer or a fumarate unit of the PLEOF macromer to form the growing primary radicals. Since mobility of the PLEOF macromer is significantly less than the NVP monomer (PLEOF with M_n of 8000–9000 Da and NVP with molecular weight of 111 Da), the growing primary radicals react with NVP monomers to form short growing chains. These short growing chains react with other fumarate units to form crosslinks between the PLEOF chains which increase the number of elastically active chains in the network. Therefore, as the initiator concentration is increased, the number (Eq. (4)) and mobility/reactivity (shorter kinetic chain length according to Eq. (5)) of the growing radicals are increased which, in turn, increase the number of crosslinks and the shear storage modulus of the hydrogel, as shown in Fig. 3, while the swelling ratio and sol fraction show a decreasing trend (Fig. 5(a)).

PLEOF hydrogels with higher hydrophobicity, i.e., higher PLA:PEG ratios, had higher sol fraction, lower modulus,

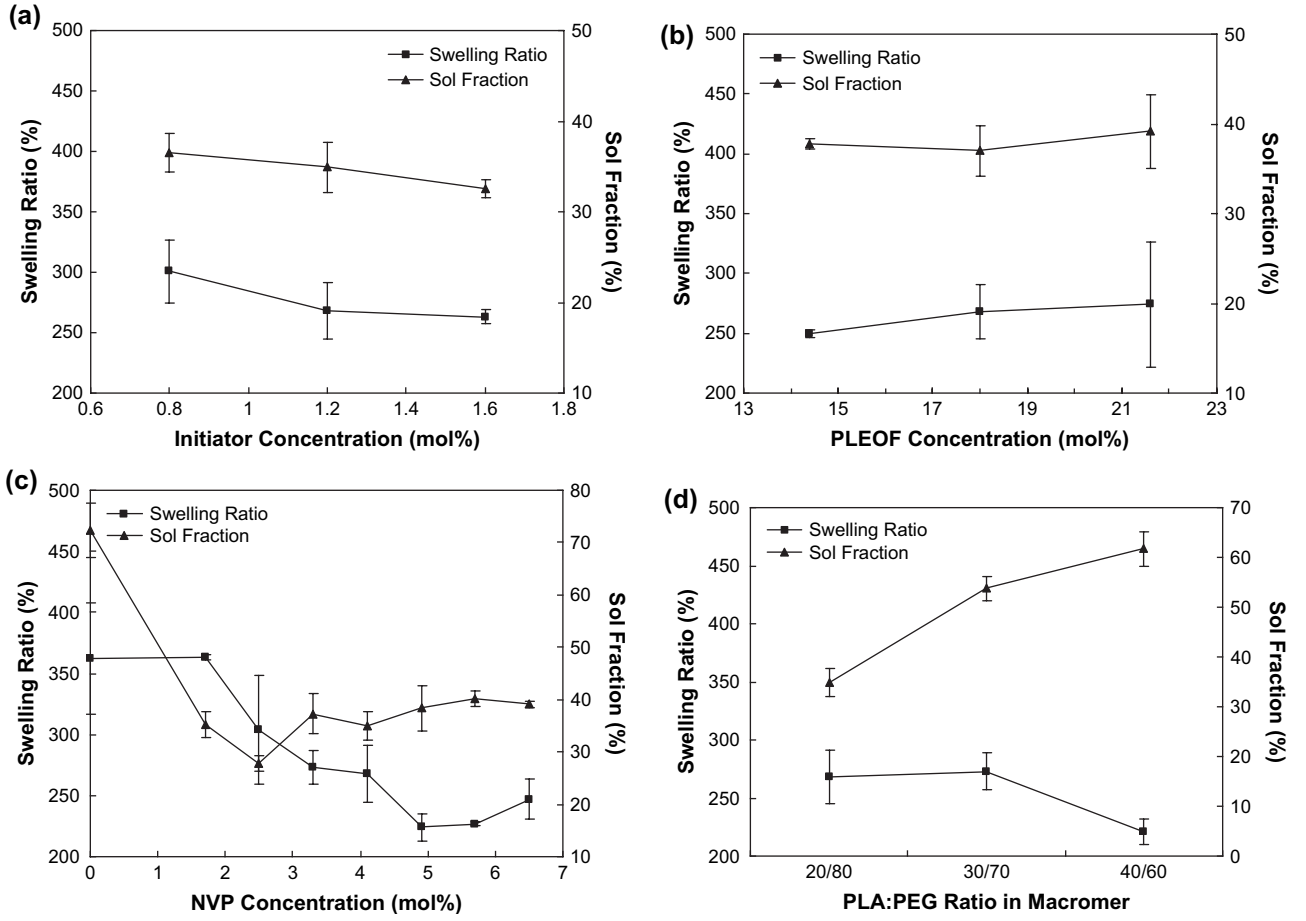

Fig. 5. Variation of the swelling ratio and sol fraction with (a) UV initiator concentration in 18.0P–4.1N hydrogels, (b) PLEOF concentration in 4.1N–1.2I hydrogels, (c) NVP concentration in 18.0P–1.2I hydrogels, and (d) PLA:PEG ratio in 18.0P–4.1N–1.2I hydrogels ($d = 10$ cm and $t_{UV} = 30$ min). The values are the mean of four samples with error bars representing one standard deviation from the mean.

and lower swelling ratio. PLEOF macromers with different PLA:PEG ratios had similar molecular weight distribution and the number of fumarate groups per chain was comparable between PLEOF samples (4–5 fumarate groups per chain). Therefore, the apparent reactivity of the fumarate groups (with growing NVP chains or other fumarate units) decreased for samples with higher PLA:PEG ratios. This can be attributed to the reduction in solubility of PLEOF macromers in aqueous media and shielding of fumarate groups by hydrophobic PLA segments (see Fig. 7). In aqueous solution, PLEOF macromers can physically crosslink by hydrophobic interactions between the lactide groups on different chains. To test for this effect, the aqueous PLEOF solution was placed as a thin film between the plates of the rheometer and heated to 60 °C. Then, the sample shear viscosity was measured with time as the sample was cooled slowly (1 °C/min) to ambient conditions. No significant change or discontinuity in sample viscosity was observed, due to hydrophobic lactide interactions, in the concentration range of 15–25 mol% PLEOF in water. Since the ethylene oxide (EG) fraction in the macromer was higher than that of the lactide, strong hydrophilic interactions (hydrogen bonding) between the water molecules and EG units favored over weaker hydrophobic (van der Waals) interactions between the lactide units on different chains. Consequently, compared to covalent crosslinking, hydrophobic lactide interactions did not play a significant role in crosslinking the PLEOF chains in aqueous solution.

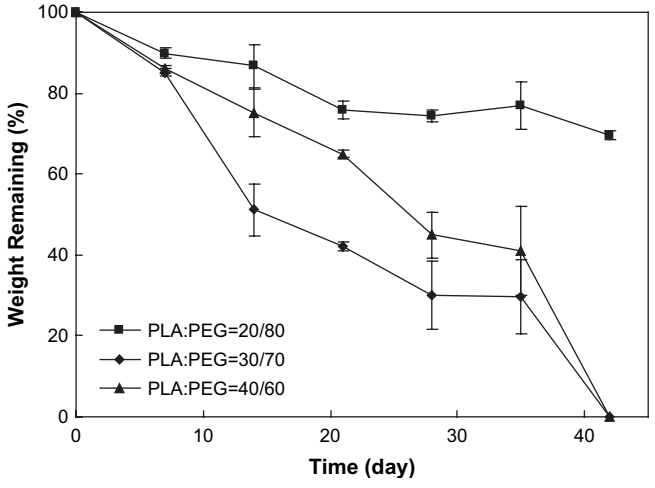

Fig. 6. Degradation of PLEOF hydrogels, expressed as the sample weight versus time, for different PLA:PEG ratios. The values are the mean of four samples with error bars representing one standard deviation from the mean.

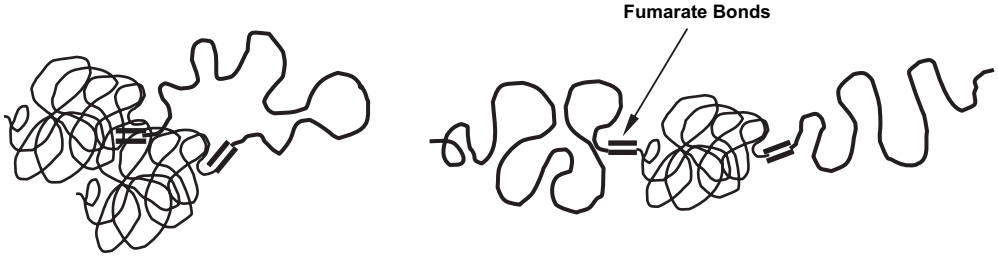

Fig. 7. Schematic diagram to illustrate the effect of PEG (thick lines) and PLA (thin lines) ratio on the structure of PLEOF macromer. In macromers with high PLA:PEG ratio (left) the reactive fumarate bonds are shielded by the high concentration of hydrophobic PLA blocks, while in macromers with low PLA:PEG ratio (right) the concentration of PLA blocks was too low to effectively shield the fumarate bonds.

Two regimes can be identified for the effect of NVP on mechanical and swelling characteristics: a low NVP regime (i.e., <4.1–4.9 mol%) in which the extent of crosslinking increased and swelling ratio decreased with increasing NVP concentration, and a high NVP regime (i.e., >4.1–4.9 mol%) where the extent of crosslinking decreased and swelling ratio increased slightly with NVP concentration. Similar effects have been observed when poly(propylene fumarate) macromer was crosslinked with diethyl fumarate monomer [49]. The effect of NVP on the structure of photo-crosslinked PLEOF hydrogels is shown schematically in Fig. 8. PLEOF macromers can crosslink even in the absence of NVP, however, the resulting PLEOF hydrogels (18.0P–0.0N–1.2I) have at least an order of magnitude lower modulus and higher sol fraction that those crosslinked with NVP. In the absence of NVP, radicals formed by UV radiation react with the unsaturated fumarate units on PLEOF chains to form the primary growing radicals. Since these radicals are attached to PLEOF chains, they have lower mobility/reactivity and a significant fraction terminates by chain transfer to solvent (water) before they can react with fumarate units on other PLEOF chains to form crosslinks.

As NVP is added to the mixture, short growing chains are produced by the reaction of primary radicals with NVP monomers which serve as the ‘‘bridge’’ to covalently crosslink the fumarate groups on PLEOF chains. This bridging mechanism incorporates additional fumarate units in the PLEOF network and forms additional elastically active crosslink points which results in higher shear modulus (Fig. 4(b)), lower swelling ratio and lower sol fraction (Fig. 5(c)). With the addition of more NVP, the shear modulus reaches a maximum because the density of growing NVP chains and chain mobility (kinetic chain length) are optimum (see Fig. 4(b)). With further addition of NVP, the kinetic chain length of the growing radicals is increased (see Eq. (5)), reducing their mobility, which reduces their ability to link the PLEOF chains. Therefore, the probability of the reaction between two growing NVP chains is increased at the expense of that between growing NVP chains and fumarate units, leading to the formation of free (soluble) or dangling NVP chains. As a result, the shear modulus is deceased (Fig. 4(b)) and swelling ratio and sol fraction are increased (Fig. 5(c)). These finding demonstrate that the reactivity of a fumarate unit with other fumarates on PLEOF chains is significantly lower than that of a fumarate with the growing NVP chains, apparently due to the lower mobility of PLEOF chains, especially in the post-gelation regime.

The degradation characteristics of PLEOF hydrogels depended on the ratio of PLA to PEG, as shown in Fig. 6. Hydrolytic degradation occurred by cleavage of the ester links in the macromer followed by dissolution of the fragments. The PLA segments of the network, which degraded by hydrolysis of the lactide monomers, had significantly higher degradation rate compared to those of PEG segments, which degraded by hydrolysis of fumarate units at PEG chain ends (lower density and slower degradation of fumarate units compared to lactide monomers). In the absence of the lactide groups in the macromer, the hydrogel can degrade by hydrolysis of the ester groups at PEG chain ends. However, the hydrolysis rate in the absence of lactide groups is very slow because the

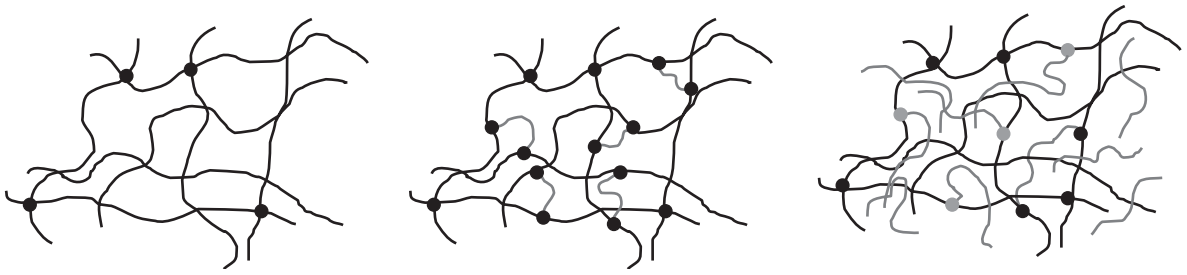

Fig. 8. Schematic diagram to illustrate the effect of NVP crosslinker on the structure of UV crosslinked PLEOF hydrogels. (Left) PLEOF macromers (black lines) crosslink via the formation of direct covalent bonds between fumarate groups (black circles), but due to low mobility of the macromers many of them cannot participate in the crosslinking reaction. (Middle) addition of NVP facilitates the reaction by forming short NVP chains (gray lines) to bridge the adjacent PLEOF chains. (Right) With increasing the amount of NVP, long NVP chains form, which are either free or attached to fumarate units at one end (gray circles). These dangling or free NVP chains reduce the mobility of the trapped PLEOF macromers and inhibit the crosslinking reaction.

concentration of degradable (ester) units is low (PEG blocks are not degradable) and the ester groups are attached to a rigid fumarate units. For example, the 18.0P–4.1N–1.2I hydrogels ($d = 10$ cm and $t_{UV} = 30$ min) had less than 5% mass loss after 12 weeks of incubation in primary culture media. With the inclusion of lactide groups to the macromer, due to significantly higher concentration of ester units (one ester group per lactide monomer) and higher reactivity (ester group attached to a more flexible lactide compared to fumarate), the hydrogel completely degraded in 6 weeks (Fig. 6). The PLEOF 20/80 (20% lactide) had the lowest degradation rate because the fraction of degradable units (lactide) was lowest, even though the swelling ratio was highest. The PLEOF 30/70 (30% lactide) had the highest degradation rate because the fraction of degradable units (lactide) and hydrophilic units (PEG) were both optimum for hydrolytic degradation.

5. Conclusion

The gelation kinetics, degradation and swelling characteristics of photo-crosslinked PLEOF hydrogels were investigated as a function of composition as well as time and intensity of UV radiation. The gelation kinetics was studied by *in situ* rheometry. The hydrogel shear modulus was directly related to time and intensity of UV exposure. The shear modulus increased when initiator concentration, PLEOF concentration, or PEG fraction of the PLEOF macromer was increased. Two regimes could be identified for the effect of NVP on mechanical and swelling characteristics: a low NVP regime (i.e., <4.1–4.9 mol%) crosslink density increased and swelling ratio decreased with increasing NVP concentration, and a high NVP regime (i.e., >4.1–4.9 mol%) where crosslink density decreased and swelling ratio increased with NVP concentration. The degradation characteristics of PLEOF hydrogel depended on the ratio of PLA to PEG. The PLEOF 30/70 (30% lactide), with optimum fraction of degradable PLA units and hydrophilic PEG units, had the highest degradation rate. *In situ* photo-crosslinked PLEOF hydrogels are attractive as a matrix for treatment of irregularly shaped defects in soft tissue engineering because they exhibit a relatively high shear modulus and water content while their degradation rate can be adjusted to fit a particular application.

Acknowledgements

This work was supported by research grants from the AO research fund of the AO (Arbeitsgemeinschaft Fur Osteosynthesefragen) Foundation (project no. 05-J95) and the Aircast Foundation.

References

[1] Trevors JT, Pollack GH. Prog Biophys Mol Biol 2005;89:1.
[2] Peppas NA, Langer R. Science 1994;263:1715.
[3] Jabbari E, Karbasi S. J Appl Polym Sci 2004;91:2862.
[4] Jabbari E, Nozari S. Eur Polym J 2000;36:2685.
[5] Peppas NA, Lustig SR. In: Peppas NA, editor. Hydrogels in medicine and pharmacy. I. Fundamentals. Boca Raton: CRC Press; 1986. p. 57.
[6] Gehrke SH, Fisher JP, Palasis M, Lund ME. Ann NY Acad Sci 1997;831:179.
[7] Monteiro MJ, Hall G, Gee S, Xie L. Biomacromolecules 2004;5:1637.
[8] Leach JB, Schmidt CE. Biomaterials 2005;26:125.
[9] Jabbari E. J Microencapsul 2004;21:525.
[10] Yamamoto M, Takahashi Y, Tabata Y. Tissue Eng 2006;12:1305.
[11] He X, Jabbari E. Biomacromolecules 2007;8:780.
[12] Karp JM, Yeh J, Eng G, Fukuda J, Blumling J, Suh KY, et al. Lab Chip 2007;7:786.
[13] Sarvestani AS, He X, Jabbari E. Biopolymers 2007;85:370.
[14] Jabbari E. Mater Res Soc Symp Proc 2006;897E:J07-03.1.
[15] Trojani C, Boukhechba F, Scimeca JC, Vandenbos F, Michiels JF, Daculsi G, et al. Biomaterials 2006;27:3256.
[16] Kim S, Healy KE. Biomacromolecules 2003;4:1214.
[17] Lutolf MP, Lauer-Fields JL, Schmoekel HG, Metters AT, Weber FE, Fields GB, et al. Proc Natl Acad Sci USA 2002;100:5413.
[18] He X, Jabbari E. Protein Pept Lett 2006;13:715.
[19] Kim P, Jeong HE, Khademhosseini A, Suh KY. Lab Chip 2006;6:1432.
[20] Mathur AM, Moorjani SK, Scranton AB. J Macromol Sci Rev Macromol Chem Phys 1996;C36:405.
[21] Kuckling D, Adler HJP, Arndt KF. ACS Symp Ser 2003;833:312.
[22] Nguyen KT, West JL. Biomaterials 2002;23:4307.
[23] Haines LA, Rajagopal K, Ozbas B, Salick DA, Pochan DJ, Schneider JP. J Am Chem Soc 2005;127:17025.
[24] Smeds KA, Pfister-Serres A, Miki D, Dastgheib K, Inoue M, Hatchell DL, et al. J Biomed Mater Res 2001;54:115.
[25] Ye Q, Spencer P, Wang Y, Misra A. J Biomed Mater Res A 2007; 80:342.
[26] Ye Q, Wang Y, Williams K, Spencer P. J Biomed Mater Res B 2007; 80:440.
[27] Hill-West JL, Chowdhury SM, Slepian MJ, Hubbell JA. Proc Natl Acad Sci USA 1994;91:5967.
[28] van de Wetering P, Metters AT, Schoenmakers RG, Hubbell JA. J Controlled Release 2005;102:619.
[29] Rydholm AE, Bowman CN, Anseth KS. Biomaterials 2005;26:4495.
[30] Davis KA, Burdick JA, Anseth KS. Biomaterials 2003;24:2485.
[31] Albertsson AC, Varma IK. Biomacromolecules 2003;4:1466.
[32] Lu S, Anseth KS. Macromolecules 2000;33:2509.
[33] Kim BS, Hrkach JS, Langer R. Biomaterials 2000;21:259.
[34] West JL, Hubbell JA. React Polym 1995;25:139.
[35] Shah NM, Pool MD, Metters AT. Biomacromolecules 2006;7:3171.
[36] Martens P, Metters AT, Anseth KS, Bowman CN. J Phys Chem B 2001;105:5131.
[37] Bryant SJ, Nuttelman CR, Anseth KS. J Biomater Sci Polym Ed 2000;11:439.
[38] Scranton AB, Bowman CN, Peiffer RW. ACS Symp Ser 1997;673:16.
[39] Fouassier J-P. Photoinitiation, photopolymerization, photocuring: fundamentals and applications. New York: Hanser Publishers; 1995.
[40] Rydholm AE, Reddy SK, Anseth KS, Bowman CN. Biomacromolecules 2006;7:2827.
[41] He S, Timmer MD, Yaszemski MJ, Yasko AW, Engel PS, Mikos AG. Polymer 2001;42:1251.
[42] Jabbari E, He X. Polym Prepr 2006;47:353.
[43] Jabbari E, He X. Polym Prepr 2006;47:192.
[44] Sarvestani AS, He X, Jabbari E. Biomacromolecules 2007;8:406.
[45] Ariff M, Jainuddin MD, Gopalan V, Venkata Rao K. J Polym Sci 1985;23:2063.
[46] Bajpai UDN, Jain A, Rai S. J Appl Polym Sci 1990;39:2187.
[47] Flory PJ, Rehner J. J Chem Phys 1943;11:512.
[48] Odian G. Principles of polymerization. New York: John Wiley; 1981. p. 210.
[49] Fisher JP, Dean D, Mikos AG. Biomaterials 2002;23:4333.